JOURNAL OF ENERGY SYSTEMS

VOLUME 2, ISSUE 4

2602-2052

DOI: 10.30521/jes.461133

Research Article

Investigation of effect of vehicle grilles on aerodynamic energy loss and drag coefficient

Ahmet Yıldız
Firat University, Faculty of Engineering, Department of Mechatronics Engineering, Elazig, Turkey,
ayildiz@firat.edu.tr
ORCID: 0000-0002-8062-2752
Beşir Dandıl
Firat University, Faculty of Technology, Department of Mechatronics Engineering, Elazig, Turkey,
bdandil@firat.edu.tr
ORCID: 0000-0002-3625-5027

Arrived: 18.09.2018 Accepted: 10.11.2018 Published: 31.12.2018

Abstract: In this study, the effects of grilles in a vehicle on the aerodynamic drag coefficient and energy loss have been investigated. For this purpose, grilles have been placed horizontally to the front of the vehicle. Firstly, the aerodynamic drag coefficient and aerodynamic energy loss of the vehicle model without grilles have been determined numerically. Then, the aerodynamic loss coefficient and the aerodynamic energy loss of the vehicle model with grilles have been determined. Thus, the effect of the grilles placed in the front of vehicle on aerodynamic resistance and energy loss is compared to the vehicle model without grilles. For all estimates, the vehicle models have been modeled in SolidWorks software. ANSYS-Fluent software has been used for numerical analysis for the modeled vehicles. It has been determined that the grilles placed in the front of vehicle increased the aerodynamic drag coefficient of the vehicle and thus the aerodynamic energy loss of the vehicle increased. Thus, it has been shown that it is possible to reduce a certain extent the additional aerodynamic losses in the vehicle by approaching the grilles designs closer to the vehicle model without grilles.

Keywords: *Vehicle, Aerodynamic drag coefficient, Energy loss, Grille, Computational fluid dynamics*

Cite this paper as: *Yildiz, A, Dandil, B. Investigation of effect of vehicle grilles on aerodynamic energy loss and drag coefficient. Journal of Energy Systems, 2018; 2(4): 190-203, DOI: 10.30521/jes.461133*

1. INTRODUCTION

The aerodynamic structure of a vehicle significantly affects the performance, control and comfort of the vehicle. By improving the aerodynamic structure of the vehicle and reducing aerodynamic drag, the performance of the vehicle is improved and fuel economy is ensured [1]. The aerodynamic force not only affects the on-road performance of the vehicle but also affects the road holding properties. The effects of aerodynamic forces are being investigated by the automobile designers. Thanks to the designs made, researchers are worked to reduce the negative effects of certain required parts such as grilles. These parts also increase the aerodynamic resistance of the vehicle [2-3]. The most important of the resistance forces that affect the vehicles is aerodynamic resistance, which significantly affects vehicle performance and fuel consumption at high speeds. A vehicle that moves at an average speed of 100 km/h spends 50-70% of its power against aerodynamic drag forces [4]. The aerodynamic drag force is increasing in direct proportion to the square of vehicle speed. Wind tunnel tests and road tests are used to improve aerodynamics in the vehicle industry. Full-scale wind tunnel tests are expensive in terms of cost. Computational fluid mechanics (CFD), which has evolved in recent years, has facilitated the calculation of complex flows around objects. The solution of the flow problems can be achieved shorter time and cheaper than the analytical method by the numerical solution method. For better understanding of the flow phenomena CFD techniques are commonly used and today almost unavoidable to include them in the machine design and testing [5]. Research on both wind tunnel tests and numerical solutions is continuing in terms of determining aerodynamic effects in vehicle design.

Experimental aerodynamic studies on land vehicles are based on the 1960s. Aerodynamic studies have been made to improve the values of drag coefficient. Aerodynamic studies have been carried out to improve the drag coefficient and thus reduce fuel consumption in the vehicles. In addition, studies are being made to improve vehicle dynamics, stability, aerodynamic sound and noise levels. Different reference models are used in the literature in aerodynamic studies [6]. The most common model in the literature is the Ahmed model [7]. Numerous experimental and numerical CFD analysis have been performed on the Ahmed model [8-9].

Wiedemann and Ewald have experimented in the wind tunnel to study the flow around the two-dimensional vehicle model. In the study, they have examined the turbulence intensity, the Reynolds number and the flow structure around the vehicle. In addition, they have determined the pressure changes around the vehicle model [10].

In an experimental study by Kramer et al., The effect of winds on the automobile was investigated experimentally and found that the side wind had a significant effect on the aerodynamic losses of the car [11].

Desai et al. (2008) have numerically and experimentally investigated the aerodynamic structure of a hybrid vehicle. Experimental studies were carried out in the open circuit wind tunnel. As a result of the experiments performed, they found the drag coefficient (C_d) and the pressure coefficient (C_p) distribution on the vehicle. In the numerical study, the drawing data of the vehicle was created in the Gambit software and analyzed in the Fluent software. They determined the drag coefficient of the vehicle as 0.4 by experimental method and 0.55 by numerical method. They stated that the numerical and experimental study results are very different according to the number of Reynolds, this difference could be due to the number of iterations and the mistakes made in the drawing [12].

Lokhande et al. (2003) investigated the aerodynamic structure of the pickup model vehicle using the Fluent package programme using LES and RNG k-ε turbulence models. It has been determined that the flow from the stone is just above the front bumper as the stagnation point [13].

Ehab Fares (2006) analyzed the 25 ° and 35 ° slant angles rear end of the vehicle in his study, numerically examined different vortex and separation behaviors in the unsteady flow, and found that the results obtained were consistent with experimental data [14].

Bayindirli (2017) was investigated aerodynamic forces effecting on combinations of trucks and trailers with computational fluids mechanics. Numerical analyzes for aerodynamic drag coefficient were done with the aid of Fluent software for 4 different free flow rates and high Reynolds numbers. The pressure based drag force distributions and drag coefficient were determined. A spoiler is designed to improve the drag force of the vehicle. With the developed spoiler, the aerodynamic drag coefficient improvement obtained by 20.9% [15].

Kataoka et al. (2008) have aimed to improve the drag resistance coefficient to improve aerodynamics structure for a particular vehicle model. In addition, they have also made efforts to improve the lift coefficient, which is an effect on driving stability. For this purpose, design modifications made with the rear spoiler and front bumper improved the drag coefficient. They also found that this design, which they had done, brought about improvements lift coefficient as well as drag coefficient [16].

Hu Xu-Xia and Wong (2011) calculated the effects of the newly developed rear spoiler on the drag and lift coefficients of the sedan car with the k-ε turbulence model in the Fluent package programme. They found that the spoilers they developed improved the drag coefficient by 1.7% and the lift coefficient by 4% [17].

Aider et al. (2009) aimed to reduce drag coefficient and lift coefficient by controlling flow separation and turbulence in the rear vortex region on Ahmed Model, a simplified vehicle model. The isosceles trapezoid shapes that they used in the rear end of Ahmed Model have found a 60% decrease in the drag coefficient and 12% in the lift coefficient [18].

Castro (2013) done RANS and DES analyses for a vehicle using ANSYS-Fluent software. Castro has repeated the tests at various speeds, thus aimed to find the drag coefficient of the vehicle more accurately by doing more iterations on different conditions. When the results were examined, it was observed that the vortex formations and flow lines realized in the rear region of the vehicle in the DES analyzes better than the RANS analyzes. When the drag coefficient of the vehicle is examined, it is stated that the DES analyzes give a slightly better result [19].

In this study, the effect of the grilles placed to the front part of a vehicle which moves at a particular speed and whose dimensions are predetermined, on the vehicle's aerodynamic drag coefficient and aerodynamic energy loss are analyzed. The Reynolds number was kept constant in the study and the velocity was assumed as 27 m / s in the analyses. Computational fluid mechanics method was used for the analysis and the solutions were analyzed by the ANSYS software.

2. METHODS

Various forces impact the movements of the vehicles. These forces acting on the vehicles are divided into the forces that provide the movement and against the movement. The force that drives the vehicle is the force produced by the engine and used as the wheel drive force. The forces that against the motion of the vehicle consist of the following resistances [20].

- Aerodynamic drag
- Gradient resistance

- Rolling resistance
- Gradient resistance
- Inertia

Generally, the drag coefficient (C_d), the lift coefficient (C_l), and the moment coefficient (C_m) are referred to the aerodynamic characteristics for the vehicle. Especially, as the drag coefficient decreases, the properties of the vehicle such as maneuver, acceleration and road holding ability are improved. In addition, as the drag coefficient decreases, the amount of energy consumed to defeat the air drag of the vehicle will also decrease, resulting in a significant reduction in fuel consumption. The aerodynamic drag coefficient is the result of flow distortions such as discontinuity and turbulence in a linear flow due to an external shape of object. If the object is exposed to the less flow disturbance in terms of the external form, consequently, the smaller the drag force and the drag coefficient. The only way to reduce the air drag loss of a vehicle whose speed and geometric dimensions are apparent is to reduce the drag coefficient (C_d), which depends on the vehicle's external shape. A schematic view of aerodynamic forces, moments, pressure and gravity centers on the car is given in Figure 1. In Figure 1, Where F_D is the drag force, F_L is the lift force, F_Y is the lateral force, M_P is the pitching moment, M_R is the rolling moment and M_Y is the yawing moment.

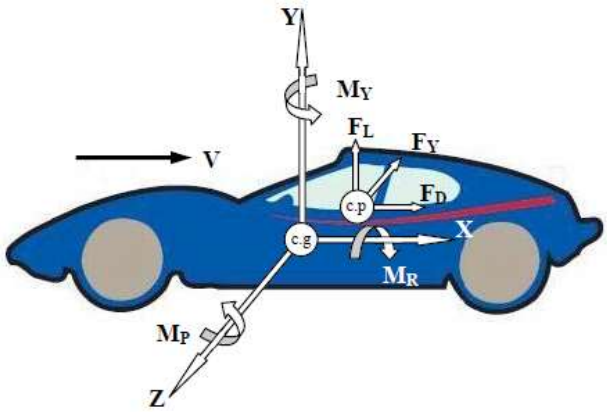

Figure 1. Aerodynamic forces, pressure and gravity centers on the car

The drag force (F_D) shown in the figure is the resistance force in the opposite direction to the forward movement direction of the vehicle. [21]. The largest component of aerodynamic force that affects road vehicles is usually the aerodynamic drag force. More than 90% of the aerodynamic drag force for a passenger vehicle is caused by form drag.

The aerodynamic forces acting to the vehicle vary depending on many parameters, mainly vehicle and environmental conditions. For this reason, the comparison process should be handled as dimensionless unit. Thus, the coefficient dimensionless expressing the resistance of the vehicle to motion is expressed as the aerodynamic drag coefficient (C_d). The aerodynamic drag coefficient is expressed as aerodynamic force (F_D), velocity of vehicle (V) and vehicle of projection area (A) as follows [22].

$$C_d = \frac{F_D}{\frac{1}{2}\rho A V^2} \tag{1}$$

The energy consumed (E_d) against the aerodynamic drag force at the distance (s) during the movement of the vehicle is expressed as in Eq. (2).

$$E_d = F_D s = \frac{1}{2}\rho A V^2 s \tag{2}$$

With the help of the equation given above, it is necessary to determine the drag coefficient in order to determine the energy loss. Computational Fluid Dynamics (CFD) is used for numerical analysis for this purpose. Accordingly, the numerical solution of a flow problem consists of the following steps:

Firstly, the governing equations which express the fluid motion in mathematical terms are determined. A system of partial differential equations is usually obtained here. Subsequently, a transformation called "discretization" is applied to these equations in order to be able to perform numerical operations. As a result of discretization; an area or volume consisting of the finite points / volumes will be created. This is the meshing. Finally, the problem is solved by determining the initial and boundary conditions. After the solution is sufficiently advanced, the results are interpreted numerically or visually.

In this study, ANSYS software is used and this software consists of three main steps.

Preprocessor: In the preprocessor, the geometry to be analyzed is created or the existing geometry is imported and the mesh process is created. The boundary conditions are also determined and the problem is made ready to be solved.

Solution: The meshing created in the preprocessor is transferred to the solution and numeric codes that are an expression of the governing equations are run on this step. It is determined which flow model the problem will be solved and the initial conditions are entered.

Postprocessor: The results of the analysis are examined numerically or visually.

In this study, SolidWorks was used as pre-processor and Ansys-Fluent software was used as solver and postprocessor.

The numerical model equations include volumetric displacement equations, mass conservation equations, cyclic temperature equations, pressure equations and energy flow relations [23]. In fluid mechanics, the governing equations which express the motion of the fluid mathematically are based on the law of conservation of mass, the law of conservation of momentum and the law of conservation of energy [24].

Reynolds Average Navier-Stokes (RANS) equations are called the Navier-Stokes equations, which are arranged according to time-averaged velocity and pressure [24-25]. The RANS equations are insufficient to form a closed system of equations. By edits for turbulent flow, six new unknowns are added to the equations. These are the Reynolds stress terms. For this reason, various turbulence models have been developed in order to complement the missing expressions. Some of these models are shown in Table 1.

Table 1. Turbulence Models

Model	
Spalart-Allmaras	RANS Based Model
k-ε	
k-ω	
Reynolds Stress Model (RSM)	
Direct Numerical Simulation (DNS)	
Large Eddy Simulation (LES)	
Detached Eddy Simulation (DES)	

In RMS-based models Spalart-Allmaras, k-ε and k-ω models, Reynolds stresses are obtained by Boussinesq approximation, whereas in RSM model, stress equations are directly solved.

The k-ε model is the most commonly used turbulence model. The k-ε model focuses on the mechanisms that influence the kinetic energy of the turbulence and makes the assumption that there is a similarity

between viscous stresses and Reynolds stresses [25]. It contains two transport equations, one is the turbulence kinetic energy (k) and the other is the turbulence dissipation rate (ε). The k-ε model has various formations as Standard, Realizable, and RNG models. This model gives good results in the free shear layers (e.g. jet flows), near-wall zone (boundary layer), and wake structure flows [26]. The standard k-ε turbulence model is used in this study.

2.1. Vehicle Geometry Modeling

In this study, the vehicle models for flow analysis have been designed by surface modeling with the help of the SolidWorks software. The dimensions of the designed vehicle models are the same. However, second vehicle model has grilles on the front surface of the vehicle while first vehicle has no grilles on the front surface of the vehicle model (Closed vehicle model). The views of the vehicle model in the SolidWorks is shown in Figure 2.

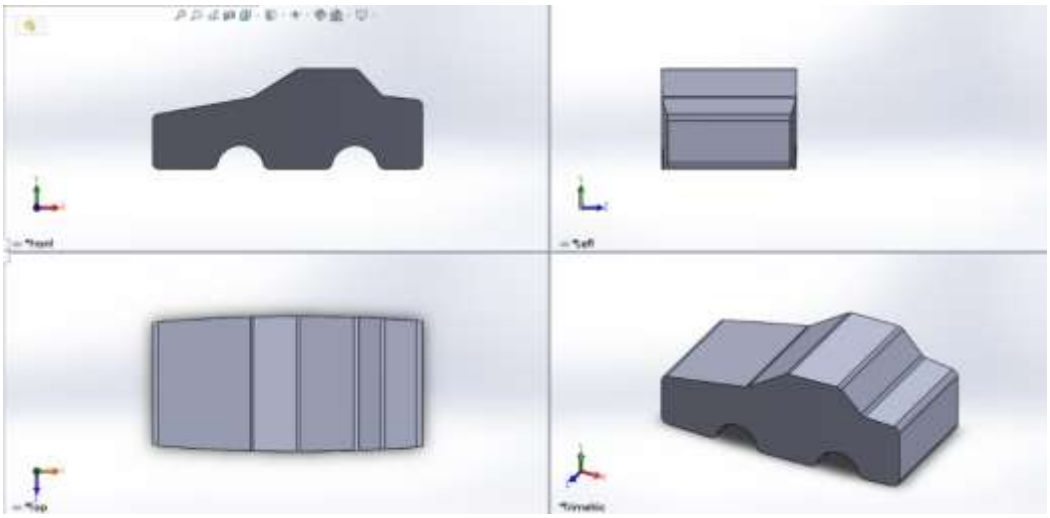

Figure 2. The views of vehicle

The front view and dimensions of the vehicle model without grilles (closed vehicle model) is given in Figure 3.

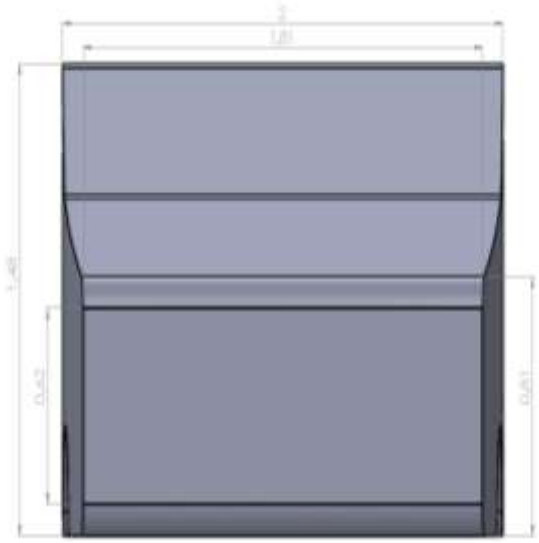

Figure 3. The front view of vehicle model without grilles

As shown in Figure 4, grilles were placed on the front surface of the closed surface model vehicle in a total area of 30 x 60 cm on the central axis.

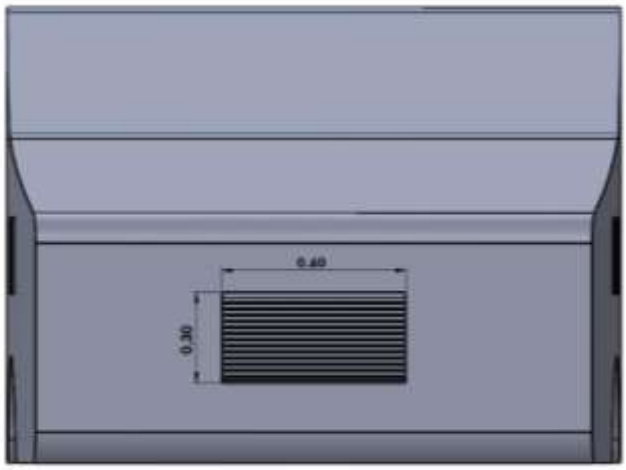

Figure 4. The front view of vehicle model with grilles

In order to discharge the air inside the hood, three air discharge grilles of 14x25 cm size are formed on the side surfaces of the vehicle as shown in Figure 5.

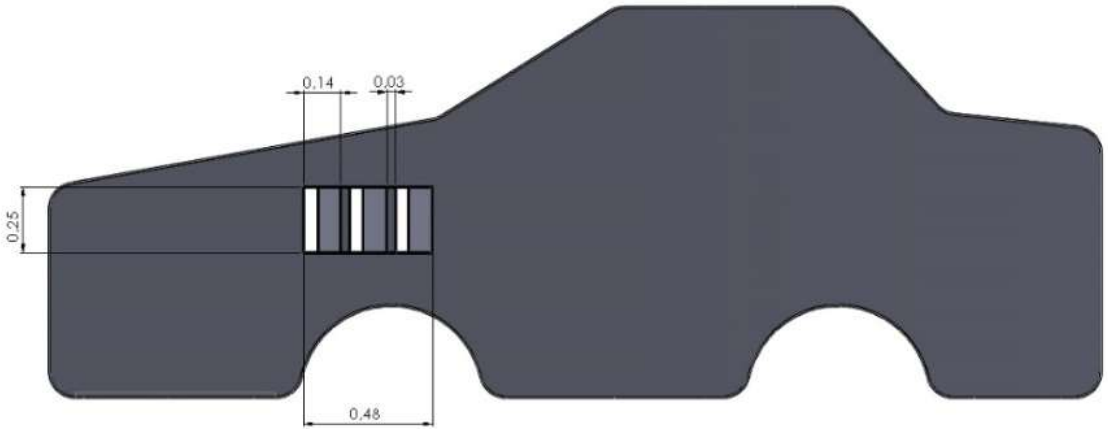

Figure 5. Air discharge grilles of vehicle model with grilles.

2.2. Wind Turbine Tunnel Creating and Mesh Generation

In order to analyze the air flow around the vehicle, a flow volume to cover the vehicle must be created. An enclosure containing the model for the flow volume is created and the volume of the vehicle is subtracted from this volume. Thus, the intersection of air and vehicle volumes is removed. This enclosure serves as an airspace. After this process, the mesh structure is created for the analysis process. Mesh processing is important so that the analyzes to be performed can yield good results. If coarse mesh structure is used for solution, efficient results cannot be obtained. In addition, the analysis solution time increases as mesh size decreases. For this reason, smaller element sizes have been used for the vehicle area where the aerodynamic drag coefficient is to be investigated, and larger element sizes have been used for the other regions. Thus, a more accurate approach has been taken in the analysis results and the solution time of the program has been reduced.

The mesh structure of the wind tunnel and the vehicle is shown in Figure 6.

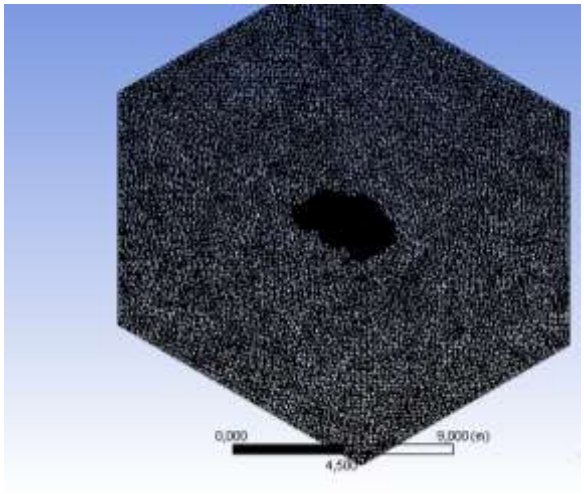

Figure 6. Mesh structure of wind tunnel and vehicle.

2.3. Boundary Conditions and Solution Setup

After the mesh operation is completed, the boundary conditions must be determined. It is important that the boundary conditions are chosen correctly so that the analysis can deliver accurate results. When the boundary conditions are determined in the ANSYS-Fluent software, the surface of the air inlet in the wind tunnel has been chosen as inlet. The surface of the air outlet has been chosen as outlet. The bottom surface has been chosen as wall. The top and side surfaces have been chosen as symmetry. Then the flow model has been chosen turbulent flow. Standard k-epsilon model has been chosen for the solution. The wall functions have been also chosen as standard. Air has been selected as the fluid in the Materials menu and the density and viscosity of the air have been taken as constant. Velocity inlet has been selected as constant 27 m/s. The pressure-speed coupling method has been selected as SIMPLE. Discretization scheme for all equations have been chosen as Second Order Upwind. The number of iterations for the analysis operations was 1000. The solution properties are given in Table 2.

Table 2. The Solution Properties

Definition	Parameters
Dimension	3D
Type	Pressure-Based
Velocity Formulation	Absolute
Time	Steady
Model	Viscous- Standard k-e, Standard Wall Function
Density (kg/m^3)	1.225
Viscosity (kg/m*s)	$1.789*10^{-5}$
Projected Surface Area (m^2)	2.96

The solution method properties are given in Table 3.

Table 3. The Solution Method Properties

Method	Properties
Scheme	SIMPLE
Gradient	Least Squares Cell Based
Pressure	Second Order
Momentum	Second Order Upwind
Turbulent Kinetic Energy	Second Order Upwind
Turbulent Dissipation Rate	Second Order Upwind

3. RESULTS

In this study, analyzes have been done for different design models taking into consideration the closed and grilles of the front part of the vehicle. In the analysis, the selected vehicle design has been modeled by taking the main dimensions constant and the solution is obtained by assuming a constant windless environment at the speed of 27 m/s in the virtual environment. All the values and properties of the solution step of each vehicle model have been taken the same. The drag force and the aerodynamic drag coefficient for the vehicle models as a result of the solution are shown in Table 4.

Table 4. Aerodynamic Drag Force and Aerodynamic Drag Coefficient for Vehicle Models.

Vehicle Model	Drag Force (N)	Drag Coefficient
Vehicle model without grilles	725.46	0.5489
Vehicle model with grilles	752.43	0.5693

When the vehicle is assumed to have travelled a distance of 100 km at a constant speed of 27 m/s, the energy consumed against the aerodynamic force has been calculated by help of Eq. (2) and is given in Fig. 7.

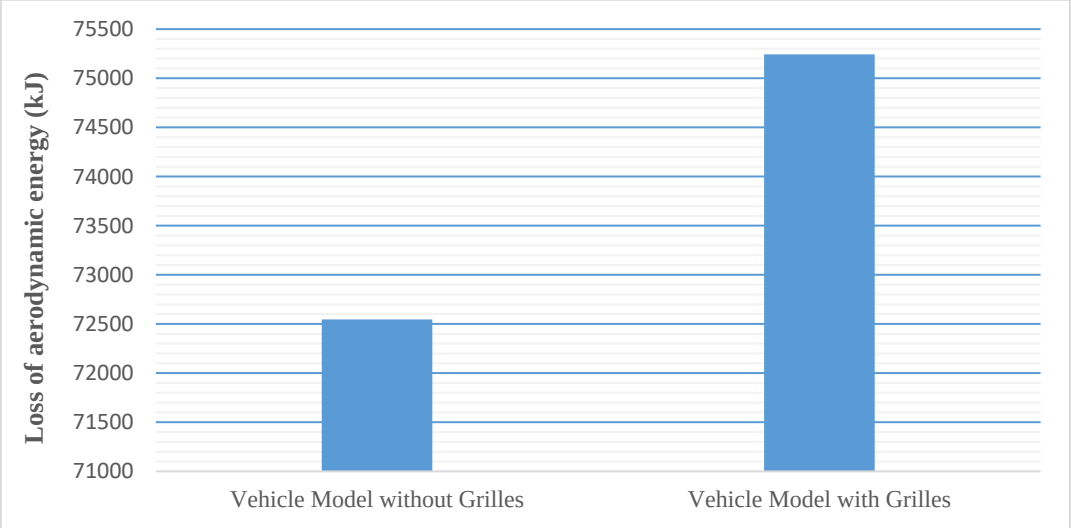

Figure 7. Amount of loss aerodynamic energy for vehicle models.

Pressure contours and velocity contours affecting the surface of the vehicles have been also obtained in the Fluent software. An isometric view of the static pressure contour of the vehicle model without grilles is given in Figure 8. When the vehicle model without grilles is compared with the vehicle model with grilles, it is seen that the stagnation point in front of the vehicle is positioned lower than vehicle model with grilles and the pressure values in the hood area are lower than vehicle model with grilles.

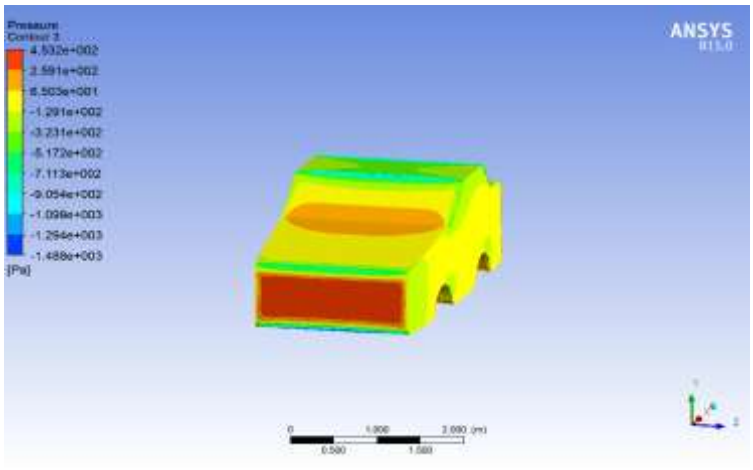

Figure 8. Pressure contours of vehicle model without grilles

Accordingly, it is seen that the maximum pressure change occurs in the front end of the vehicle. An isometric view of the static pressure contour of the vehicle model with grilles is shown in Figure 9.

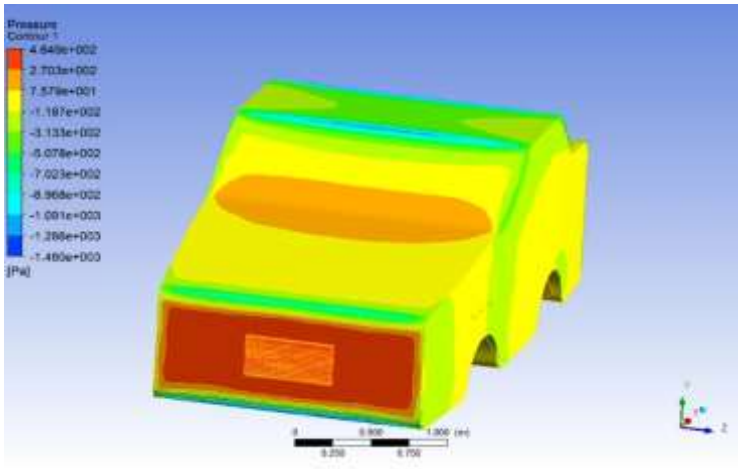

Figure 9. Pressure contours of vehicle model with grilles

Side views of the pressure contour from the cross section taken along the z-axis of the vehicle models are given in Figures 10-11.

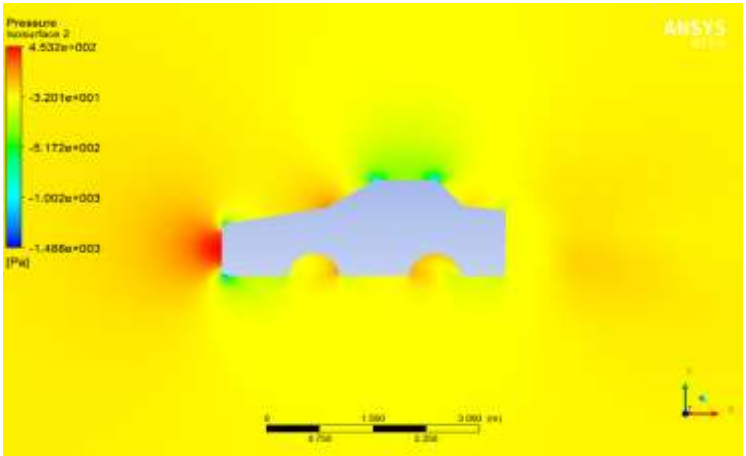

Figure 10. Side view of the pressure contour of vehicle model without grilles

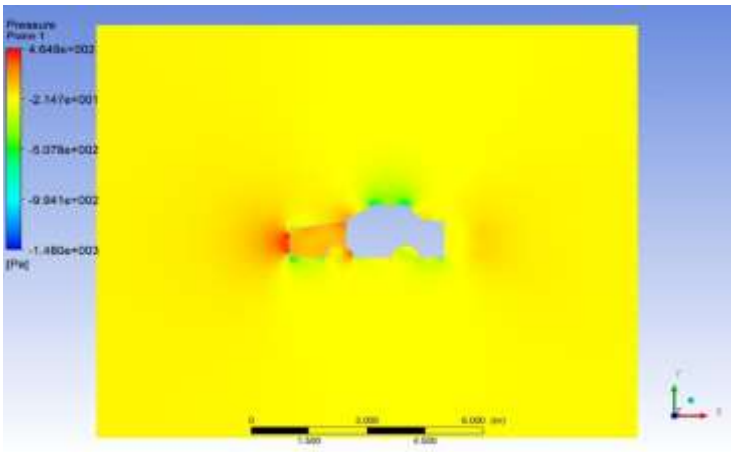

Figure 11. Side views of the pressure contour of vehicle model with grilles

The views of velocity streamlines of vehicle models are shown in Figure 12-13.

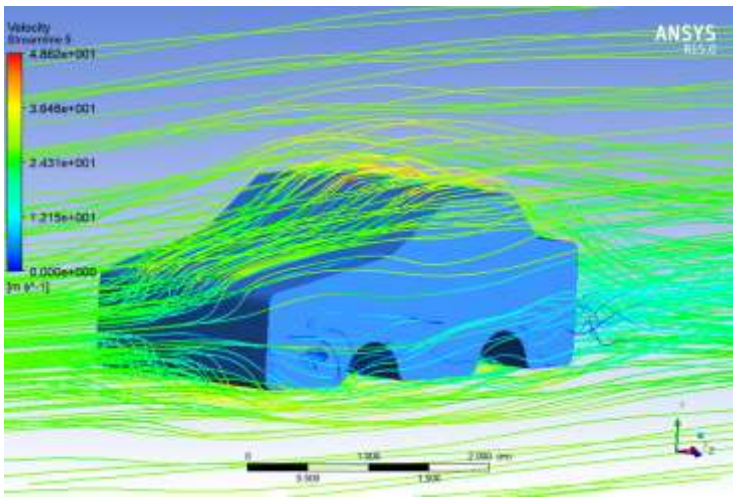

Figure 12. Isometric views of the velocity streamlines of vehicle model without grilles

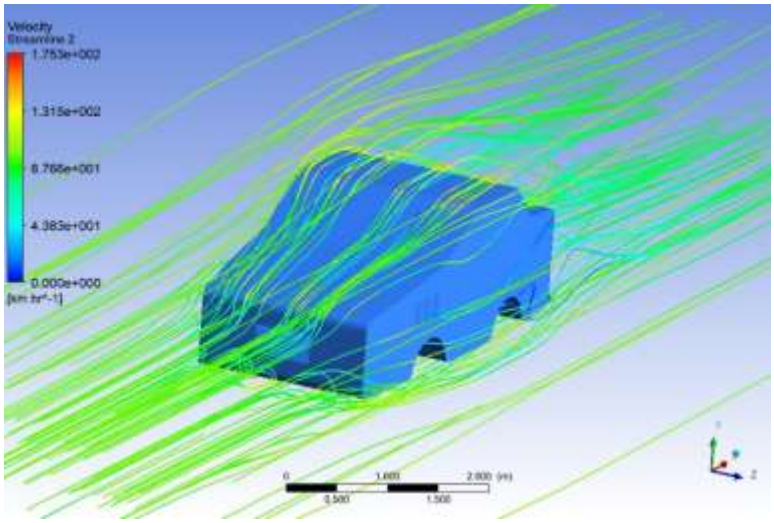

Figure 13. Isometric views of the velocity streamlines of vehicle model with grilles

In addition, the side views of the velocity contour of the cross-section taken along the z-axis of the vehicle models are given in Figures 14-15.

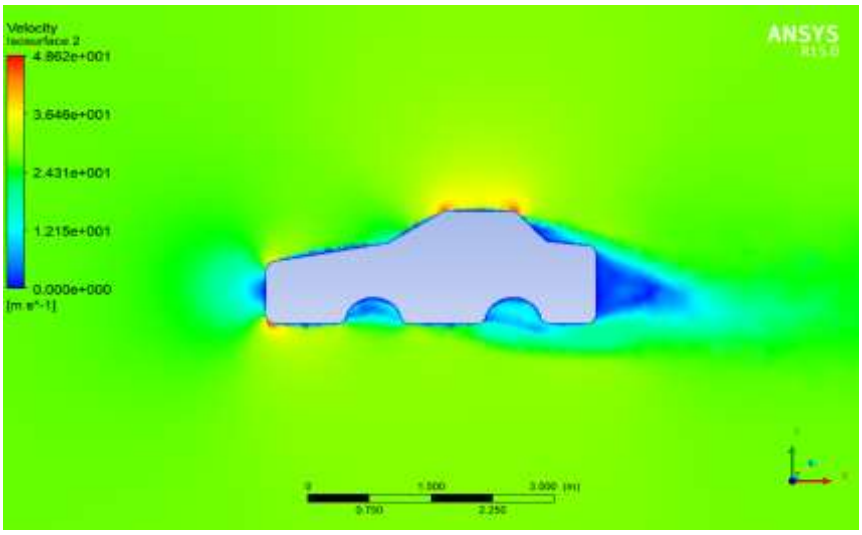

Figure 14. Isometric views of the velocity streamlines of vehicle model without grilles

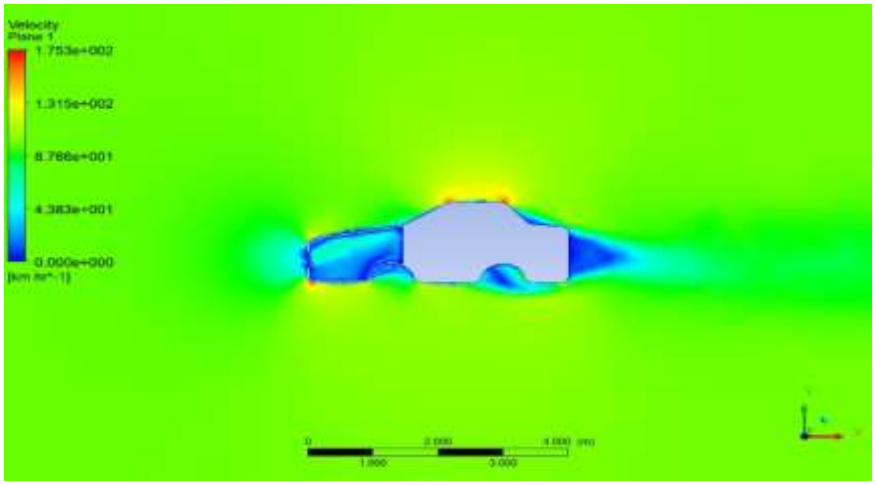

Figure 15. Isometric views of the velocity streamlines of vehicle model without grilles

When the figures are examined, it is seen that the stagnation point is at the front end of the vehicle model. As shown in the figures, a high velocity zone is formed on the hood and top of the vehicle. In addition, a low velocity zone is formed as a result of the flow separation in the area between the hood and the top of vehicle. A low velocity zone is formed because of the slowing or stopping of the air flow over the front end of the vehicle. At the rear end of the vehicle a lower velocity flow zone is occurred because of flow separation. Also under the vehicle, a high velocity zone is formed due to the resulting flow limitation. Accordingly, there was an increase of 3.71% in the aerodynamic drag coefficient due to the pressure applied to the vehicle front part in the vehicle model with grilles and the increase in the force applied to the vehicle in the flow direction.

When the speed contours were examined, it was seen that in the vehicle model with grilles, the grilles caused an increase in the amount of air directed under the vehicle and therefore the vortices that occurred behind the grilles increased. The flow occurring behind the grilles is formed of vortices of complex and different sizes. These vortices grow in size as they move downstream but their values continue to decrease in general.

The pressure difference between the front and the rear of the grilles have been resulted in a loss of energy in the flow and a velocity difference. Due to the velocity difference between the free flow velocity at the front end of the vehicle model with grilles and the grille rear region, a slip layer is formed between these two zones. There is vortex shedding in the grilles region along this sliding layer. These vortices, which turn later, cause a turbulent and irregular flow structure.

As can be seen from the figures, static pressure contours on all surfaces of the vehicle body are shown. Due to the flow stagnation at the front end of the vehicle, the air tried to escape to the sides, and therefore the static pressure of the air at the sides of the vehicle decreased. The air decreased pressure while passing over the hood of the vehicle, but there was a rapid increase in pressure when it reached the windshield. The air having high pressure at the start of the windshield accelerated as it passed through the windshield and thus the pressure decreased.

It has been observed that low pressure zones are formed in the regions where high velocities occur on vehicle models. Here, it is understood that the Bernoulli Equation is provided between the flow rate and the pressure. According to the Bernoulli Equation, because the flow stops or decelerates on the front end of the vehicle, the velocity reduced to a minimum and the pressure increased to the maximum.

4. CONCLUSION

In this study, the full scale 3D vehicle models have been modeled using SolidWorks software, and different designs have been made according to the case where the front part of vehicle is closed and grilles. For vehicle models, analyzes have been done with the aid of the Fluent software. In the analyzes, the vehicle has been assumed to travelled distance of 100 km with a constant vehicle speed of 27 m/s. Drag coefficients have been observed for the designed models and the effect of this coefficient on aerodynamic energy consumption has been investigated, and the results obtained are listed as follows.

In the analyzes, flow visualization based pressure and velocity contours and velocity streamlines have been obtained in both models, the drag coefficient has been determined and aerodynamic energy loss has been determined depending on the boundary condition.

When the pressure contour for the analyzed vehicle configurations are examined, it has been observed that there is more pressure on the front surfaces of vehicle where there is direct contact with the wind during the movement of the vehicle. It has seen that the pressure in the front part of the vehicle model without grilles is lower than the vehicle model with grilles. This configuration will provide superior performance especially in high speed conditions of the vehicle.

It has seen that the streamlines tend to surround the shape of the vehicle. It has been observed that the stream lines in the vehicle model without grilles configuration have more regular shape. Especially at high speeds, increased airflow uniformity on the vehicle surface will benefit the vehicle in terms of performance.

It has been determined that the grilles placed in the front of the vehicle caused local separation in the flow and this produced large turbulence density. It has been observed that the separated flow in the front section creates a non-symmetrical complex flow behind the grilles. This situation caused an increase in the aerodynamic drag coefficient.

According the Fluent software data, the aerodynamic drag coefficient of the vehicle model with grilles increased by about 3.71% compared to the vehicle model without grilles.

The aerodynamic energy loss of the vehicle model without grilles is observed approximately 3.7% better improvement than the vehicle model with grilles.

As a result, it can be said that vehicle performance and total fuel economy will be improved by reducing drag coefficient with vehicle model without grilles, which will lead to a significant improvement in terms of environmental pollution reduction.

REFERENCES

[1] Siva, G., Loganathan, V. Design and Aerodynamic Analysis of a Car to Improve Performance. Middle-East Journal of Scientific Research 2016; 24: 133-140

[2] Zhang, X., Toet, W., Zerihan, J. Ground effect aerodynamics of race cars. Applied Mechanics Reviews 2006; 59: 33-49.

[3] Kyle, C. R., Weaver, M. D. Aerodynamics of human-powered vehicles. Proceedings of the Institution of Mechanical Engineers, Part A: Journal of Power and Energy 2004; 218: 141-154.

[4] Modi, V. J., Hill, S. S., Yokomizo, T. Drag reduction of trucks through boundary-layer control. Journal of wind engineering and industrial aerodynamics 1995; 54: 583-594.

[5] Fernandez-Gamiz, U., Demirci, M., İlbaş, M., Zulueta, E., Ramos, J. A., Lopez-Guede, J. M., Kurt, E. Computational characterization of an axial rotor fan. Journal of Energy Systems 2017; 1(4): 129-137.

[6] Le Good, G. M., Garry, K. P. On the use of reference models in automotive aerodynamics. SAE Technical Paper, 2004.

[7] Ahmed, S. R., Ramm, G., Faltin, G. Some salient features of the time-averaged ground vehicle wake. SAE Transactions, 1984.

[8] Gilliéron, P., Leroy, A., Aubrun, S., Audier, P. Influence of the slant angle of 3D bluff bodies on longitudinal vortex formation. Journal of Fluids Engineering 2010; 132(5): 051104.

[9] Rajsinh, C., Raj, T. K. Numerical Investigation of External Flow around the Ahmed Reference Body Using Computational Fluid Dynamics. Research Journal of Recent Sciences 2012; 9: 1-5.

[10] Wiedemann, J., Ewaldt, B. Turbulence manipulation to increase effective Reynolds numbers in vehicle aerodynamics. AIAA journal 1989; 27: 763-769.

[11] Kramer, C., Grundmann, R., Gerhardt, H. J. Testing of road vehicles under cross wind conditions. Journal of Wind Engineering and Industrial Aerodynamics 1991; 38(1): 59-69.

[12] Desai, M., Channiwala, S. A., Nagarsheth, H. J. Experimental and computational aerodynamic investigations of a car. WSEAS Transactions on Fluid Mechanics 2008; 4(3): 359-366.

[13] Lokhande, B., Sovani, S., Khalighi, B. Transient simulation of the flow field around a generic pickup truck. SAE Technical Paper, 2003

[14] Fares, E. Unsteady flow simulation of the Ahmed reference body using a lattice Boltzmann approach. Computers & Fluids 2006; 35(8-9): 940-950.

[15] Bayindirli, C. The Analysis of the Effect of the Spoiler Structures on the Truck Trailer Vehicle to Coefficient Drag by Computational Fluid Mechanics, Journal of Polytechnic, 2017; 20 (2): 251-256

[16] Kataoka, S., Hashimoto, N., Yoshida, M., Kimura, T., Hamamoto, N. Aerodynamics for Lancer Evolution X. Mitsubishi Motors Technical Review 2008; 20: 38-41.

[17] Hu, X. X., Wong, T. T. A numerical study on rear-spoiler of passenger vehicle. World Academy of Science, Engineering and Technology 2011; 57: 636-641

[18] Aider, J. L., Beaudoin, J. F., Wesfreid, J. E. Drag and lift reduction of a 3D bluff-body using active vortex generators. Experiments in fluids 2010; 48(5): 771-789.

[19] Castro, N., Lopez, O. D., Munoz, L. Computational prediction of a vehicle aerodynamics using detached Eddy simulation. SAE International Journal of Passenger Cars-Mechanical Systems 2013; 6: 414-423.

[20] Hucho, W.H. Aerodynamics of Road Vehicles: From Fluid Mechanics to Vehicle Engineering, 4th Edition, the University Press, Cambridge, London, 1990

[21] Heisler, H. Advanced Vehicle Technology, Second Edition, Reed Educational and Professional Publishing Ltd., Oxford, 2002

[22] Yildiz, A., Dandil, Beşir. Recovery of a Vehicle's Energy Loss by the Wind Turbine. In: ECRES 2018 6. European Conference on Renewable Energy System; 25-27 June 2018, Istanbul, Turkey

[23] Shufat, S. A. A., Kurt, E., El Hadad, K. M., Hancerlioğulları, A. A numerical model for a Stirling engine. Journal of Energy Systems 2018; 2(1): 1-12.

[24] Tu, J., Yeoh, G. H., Liu, C. Computational fluid dynamics: a practical approach. Butterworth-Heinemann, 2008

[25] Versteeg, H. K., Malalasekera, W. An introduction to computational fluid dynamics: the finite volume method. Pearson Education, 2007

[26] Dick, E., Kubacki, S. Transition models for turbomachinery boundary layer flows: A review. International Journal of Turbomachinery, Propulsion and Power 2017; 2(2): 4.